Available online at www.sciencedirect.com
SCIENCE DIRECT®
Physica C 417 (2005) 103–109
PHYSICA C
www.elsevier.com/locate/physc

An alternative interpretation of the magnetic penetration depth data on $Pr_{2-x}Ce_xCuO_{4-y}$ and $La_{2-x}Ce_xCuO_{4-y}$

K.-K. Voo [a,*], W.C. Wu [b]

[a] Department of Electrophysics, National Chiao Tung University, 1001 Ta-Hsueh Rd., Hsinchu 300, Taiwan
[b] Department of Physics, National Taiwan Normal University, Taipei 11650, Taiwan

Received 22 September 2004; received in revised form 15 October 2004; accepted 15 October 2004
Available online 21 November 2004

Abstract

We have revisited the magnetic penetration depth data on the electron-doped cuprates, $Pr_{2-x}Ce_xCuO_{4-y}$ and $La_{2-x}Ce_xCuO_{4-y}$. It is proposed that the transition between nodal-gap-like and nodeless-gap-like behavior upon electron-doping [e.g., see M. Kim et al., Phys. Rev. Lett. 91 (2003) 87001] can be due to a scattering of the quasiparticles in the d-wave superconducting state by an incipient or weak antiferromagnetic spin-density-wave. This conjecture is supported by the inelastic neutron scattering and angle-resolved photoemission experiments on some closely related electron-doped cuprates.

PACS: 74.72.−h; 74.20.Rp; 74.20.Mn

1. Introduction

A common opening sentence in papers related to the high-T_c cuprates is, "After fifteen years of its discovery, the mechanism of superconductivity in the high-T_c cuprates is still under debate...". Meanwhile, an intimately related question, the symmetry of the superconductivity order also still possess some ambiguity, and nailing down the gap symmetry can make a tread for attempts to unveil the superconducting (SC) mechanism. Today's situation is that, in the hole-doped (h-doped) compounds, tetragonally symmetric $d_{x^2-y^2}$-wave superconductivity (dSC) is obtained unanimously in the underdoped and optimally-doped compounds [1]. In the overdoped compounds, diverged results like fully gapped d + *i*s, d + *i*d′ [2] or orthorhombic $d_{x^2-y^2}$ + s [3] may be obtained by different probes. For the electron-doped (e-doped) compounds, observations are more converged. A nodal SC gap, most probably $d_{x^2-y^2}$ [4], is observed at underdoped. Upon electron-doping, a nodeless

* Corresponding author. Tel.: +886 3 571 2121x56176; fax: +886 3 572 5230.
E-mail address: kkvoo@cc.nctu.edu.tw (K.-K. Voo).

0921-4534/$ - see front matter
doi:10.1016/j.physc.2004.10.011

gap is developed as seen in the magnetic penetration depth (MPD) measurement [5–10]. Moreover, the gap may become nodal again at overdoped [10]. The symmetry of the nodeless gap is controversial and various possibilities have been proposed [11–13], such as a conventional s-wave, or some unconventional symmetry waves like $p + ip'$ [14]. If one admits that the symmetry of the e-doped compounds could indeed differ from its h-doped partner and transmutation of gap symmetry does occur, such a situation will be bewildering. It seems that there are different mechanisms of superconductivity governing the e-doped and h-doped cuprates. Moreover, a quantum phase transition (QPT) or more QPTs may be taking place in the e-doped cuprates. We think that the diverging observations of the h-doped cuprates at the overdoped regime are due to difficulties in the individual experiments, but the more converged result of the e-doped compounds needs to be seriously look into.

More often the transition between nodal-gap and nodeless-gap behavior in the MPD, on which most conclusions of a gap symmetry transition are based, is ascribed to a QPT of some origin [14]. In this Letter, we have chosen a more conservative but phenomenological approach. We take two observational facts as the input. A caveat beforehand is that those observations are not on the compounds which the MPD data were taken, due to the fact that a particular experimental probe usually does not access different compounds equally well. Nevertheless, those observations are on the e-doped compounds. The first observation is due to the inelastic neutron scattering (INS) experiment, by which a soft-frequency and momentum $\mathbf{q} = \mathbf{Q} \equiv (\pi,\pi)$ (commensurate) scattering is observed in the $Nd_{2-x}Ce_xCuO_4$ compounds [15,16]. [1] The presence of such a soft excitation in contrast to the h-doped cuprates is in congruence with the fact that the antiferromagnetic (AF) phase is more robust in the e-doped cuprates, and destroyed only at higher doping levels [17]. The second observation is due to the angle-resolved photoemission spectroscopy (ARPES) on the Nd compounds. A pseudogap is seen to open up at the intersections of the AF magnetic Brillouin zone (MBZ) boundary and the Fermi surface (FS) [18]. The scattering that is responsible for the pseudogap thus has momentum (π,π) and is sharp in momentum space. Putting the INS and ARPES observations together, we propose that in those e-doped cuprates where the MPD data were taken, there also exists a soft magnetic fluctuation with momentum (π,π) and it is coupled to the quasiparticles.

[1] Whereas in the h-doped cuprates, a commensurate INS peak also exists but is resonance-like and at higher energies.

2. Formulation and results

We will study a model system with dSC coexisting with a *weak* AF spin-density wave (SDW). The weak SDW order is used to model an *incipient* SDW, or a soft-energy, momentum $\mathbf{q} = \mathbf{Q}$ magnetic fluctuation. An implicit assumption in this approximation is, all vertex corrections in the current-current correlation function (which is related to the MPD) are neglected, and only the self-energy which directly affects the quasiparticle (QP) spectrum is considered. As shown by Kampf and Schrieffer [19], the change in the single-particle spectrum due to a static SDW was essentially the same as that due to the scattering by a long coherence length, soft magnetic fluctuation (see also Ref. [20]). Thus this modeling should be physically sound for the current problem.

We start from a hamiltonian with dSC and AF SDW order,

$$H = \sum_{\mathbf{k}\sigma} \xi_{\mathbf{k}} c^{\dagger}_{\mathbf{k}\sigma} c_{\mathbf{k}\sigma} + \sum_{\mathbf{k}} [\Delta_{\mathbf{k}} c^{\dagger}_{\mathbf{k}\uparrow} c^{\dagger}_{-\mathbf{k}\downarrow} + \text{H.c.}] + \sum_{\mathbf{k}\sigma} \Phi\sigma c^{\dagger}_{\mathbf{k}\sigma} c_{\mathbf{k}+\mathbf{Q}\sigma}, \quad (1)$$

where $\xi_{\mathbf{k}} = -2t(\cos k_x + \cos k_y) - 4t' \cos k_x \cos k_y - \mu$, t is the nearest-neighbor (NN) hopping which is set to 1, $t' = -0.4$ is the next-nearest-neighbor (NNN) hopping used to reproduce a typical bowed FS, $\mathbf{Q} \equiv (\pi,\pi)$, $\sigma = +1\ (-1)$ for spin up (down), μ is the chemical potential, and $\Delta_{\mathbf{k}}$ and Φ are the SC and SDW order respectively. For a particular band filling, a fixed μ is used at all temperatures, superconducting and normal states. The slight change of μ is below one percent in all our cases, and is neglected. All equations in this paper are derived for a

complex-valued $\Delta_{\mathbf{k}}$ and a real-valued Φ, but we will be discussing only the $d_{x^2-y^2}$-symmetry SC state, i.e., $\Delta_{\mathbf{k}} = \Delta_{\mathbf{k}}^* \equiv \Delta_{SC}(\cos k_x - \cos k_y)/2$. The values of Δ_{SC} and Φ in our context are not solved in the usual mean field manner, but they are *chosen*. We have chosen $\Delta_{SC} = 0.1$ and $\Phi = 0.2$ [2] throughout this paper, and the resulting system is metallic (in accord with the real materials).

Defining a Nambu operator

$$\Psi_{\mathbf{k}} \equiv \begin{bmatrix} c_{\mathbf{k}\uparrow} \\ c^{\dagger}_{-\mathbf{k}\downarrow} \\ c_{\mathbf{k}+\mathbf{Q}\uparrow} \\ c^{\dagger}_{-\mathbf{k}-\mathbf{Q}\downarrow} \end{bmatrix}, \tag{2}$$

one can then define a 4×4 Matsubara Green function matrix $G(\mathbf{k},\tau)$ component-wise by $[G(\mathbf{k},\tau)]_{\alpha\beta} \equiv -\langle T_\tau \Psi_{\mathbf{k}\alpha}(\tau)\Psi_{\mathbf{k}\beta}{}^{\dagger}\rangle$. The temporal-Fourier-transformed SC Green function matrix $G^{SC}(\mathbf{k},i\omega_n)$ is found to be

$$G^{SC}(\mathbf{k}, i\omega_n) = \sum_{\eta,\sigma=\pm 1} \frac{a^{SC}_{\eta\sigma}(\mathbf{k})}{i\omega_n - E_{\eta\sigma}(\mathbf{k})}, \tag{3}$$

where $a^{SC}_{\eta\sigma}(\mathbf{k})$ is the hermitian spectral weight matrix whose components are

$$\begin{aligned}
[a^{SC}_{\eta\sigma}(\mathbf{k})]_{11} &= \frac{\sigma}{2[E_+(\mathbf{k})^2 - E_-(\mathbf{k})^2]}\left[\left[1 + \frac{\xi_{\mathbf{k}}}{E_{\eta\sigma}(\mathbf{k})}\right]\right. \\
&\quad \times [E_{\eta\sigma}(\mathbf{k})^2 - E^2_{\mathbf{k}+\mathbf{Q}} - \Phi^2] \\
&\quad \left. + \frac{\Phi^2}{E_{\eta\sigma}(\mathbf{k})}(\xi_{\mathbf{k}} + \xi_{\mathbf{k}+\mathbf{Q}})\right], \\
[a^{SC}_{\eta\sigma}(\mathbf{k})]_{12} &= \frac{\sigma}{2[E_+(\mathbf{k})^2 - E_-(\mathbf{k})^2]E_{\eta\sigma}(\mathbf{k})} \\
&\quad \times [\Delta_{\mathbf{k}}[E_{\eta\sigma}(\mathbf{k})^2 - E^2_{\mathbf{k}+\mathbf{Q}}] + \Delta_{\mathbf{k}+\mathbf{Q}}\Phi^2], \\
[a^{SC}_{\eta\sigma}(\mathbf{k})]_{13} &= \frac{\sigma\Phi}{2[E_+(\mathbf{k})^2 - E_-(\mathbf{k})^2]} \\
&\quad \times \left[\frac{1}{E_{\eta\sigma}(\mathbf{k})}[E_{\eta\sigma}(\mathbf{k})^2 - \Phi^2 + \xi_{\mathbf{k}}\xi_{\mathbf{k}+\mathbf{Q}}\right. \\
&\quad \left. + \Delta_{\mathbf{k}}\Delta^*_{\mathbf{k}+\mathbf{Q}}] + (\xi_{\mathbf{k}} + \xi_{\mathbf{k}+\mathbf{Q}})\right],
\end{aligned}$$

$$\begin{aligned}
[a^{SC}_{\eta\sigma}(\mathbf{k})]_{14} &= \frac{\sigma\Phi}{2[E_+(\mathbf{k})^2 - E_-(\mathbf{k})^2]E_{\eta\sigma}(\mathbf{k})} \\
&\quad \times [E_{\eta\sigma}(\mathbf{k})(\Delta_{\mathbf{k}} + \Delta_{\mathbf{k}+\mathbf{Q}}) \\
&\quad + \xi_{\mathbf{k}}\Delta_{\mathbf{k}+\mathbf{Q}} - \xi_{\mathbf{k}+\mathbf{Q}}\Delta_{\mathbf{k}}].
\end{aligned} \tag{4}$$

$[a^{SC}_{\eta\sigma}(\mathbf{k})]_{22}$, $[a^{SC}_{\eta\sigma}(\mathbf{k})]_{23}$, and $[a^{SC}_{\eta\sigma}(\mathbf{k})]_{24}$ are obtained from $[a^{SC}_{\eta\sigma}(\mathbf{k})]_{11}$, $[a^{SC}_{\eta\sigma}(\mathbf{k})]_{14}$, and $[a^{SC}_{\eta\sigma}(\mathbf{k})]_{13}$ respectively by the substitution $\xi_{\mathbf{k}} \to -\xi_{\mathbf{k}}$, $\xi_{\mathbf{k}+\mathbf{Q}} \to -\xi_{\mathbf{k}+\mathbf{Q}}$, $\Delta_{\mathbf{k}} \to \Delta^*_{\mathbf{k}}$, $\Delta_{\mathbf{k}+\mathbf{Q}} \to \Delta^*_{\mathbf{k}+\mathbf{Q}}$; while $[a^{SC}_{\eta\sigma}(\mathbf{k})]_{33}$, $[a^{SC}_{\eta\sigma}(\mathbf{k})]_{34}$, and $[a^{SC}_{\eta\sigma}(\mathbf{k})]_{44}$ are obtained from $[a^{SC}_{\eta\sigma}(\mathbf{k})]_{11}$, $[a^{SC}_{\eta\sigma}(\mathbf{k})]_{12}$, and $[a^{SC}_{\eta\sigma}(\mathbf{k})]_{22}$ respectively by the exchange $\xi_{\mathbf{k}} \leftrightarrow \xi_{\mathbf{k}+\mathbf{Q}}$, $\Delta_{\mathbf{k}} \leftrightarrow \Delta_{\mathbf{k}+\mathbf{Q}}$. The poles are $E_{\eta\sigma}(\mathbf{k}) \equiv \eta E_\sigma(\mathbf{k})$ (η, $\sigma = \pm 1$), with

$$\begin{aligned}
E_\sigma(\mathbf{k}) \equiv \left\{ \frac{E^2_{\mathbf{k}} + E^2_{\mathbf{k}+\mathbf{Q}}}{2} + \Phi^2 + \sigma\left\{\left(\frac{E^2_{\mathbf{k}} - E^2_{\mathbf{k}+\mathbf{Q}}}{2}\right)^2\right.\right. \\
\left.\left. + \Phi^2[(\xi_{\mathbf{k}} + \xi_{\mathbf{k}+\mathbf{Q}})^2 + |\Delta_{\mathbf{k}} + \Delta_{\mathbf{k}+\mathbf{Q}}|^2]\right\}^{1/2}\right\}^{1/2},
\end{aligned} \tag{5}$$

where $E_{\mathbf{k}} \equiv (\xi_{\mathbf{k}}{}^2 + |\Delta_{\mathbf{k}}|^2)^{1/2}$. Note that for the current case $\Delta_{\mathbf{k}+\mathbf{Q}} = -\Delta_{\mathbf{k}}$ and the term $|\Delta_{\mathbf{k}} + \Delta_{\mathbf{k}+\mathbf{Q}}|$ in $E_\sigma(\mathbf{k})$ vanishes, but is kept for better illustration. Each SC branch is splitted by the SDW or vice versa speaking, forming four branches of excitations $E_{\eta\sigma}(\mathbf{k})$.

A few more words on what we mean by a weak SDW is desired. Fig. 1(a) shows the normal state DOS for cases of different magnitudes of the SDW order, and it is seen that for our band with a weak SDW, no gap is formed at any chemical potential in contrast to the strong SDW case. Nevertheless, the FS may still be fragmented at some band fillings as seen in the distribution of near-Fermi-level spectral weight [Fig. 1(b) and (c)]. The near-Fermi-level spectral weight as a function of momentum is defined by $A(\mathbf{k}) \equiv \int_{-0.15|t|}^{+0.15|t|} d\omega\pi^{-1} \times \mathrm{Im}G^{SC}_{11}(\mathbf{k}, \omega + i0) f(\omega)$, where $f(\omega)$ is the Fermi distribution function but here it is taken as the Heaviside step function $\Theta(-\omega)$ for $T = 0$ limit. The integration limit "$0.15|t|$" is an arbitrarily chosen small parameter, which is larger than Δ_{SC} however.

[2] In the sense of the usual mean-field theory, $\Phi = U\langle S_z\rangle$, where U is the onsite Hubbard repulsion and S_z is the z-component of the spin operator. Therefore $\Phi = 0.2$ and $U \sim 5$ implies $\langle S_z\rangle \sim 0.04$.

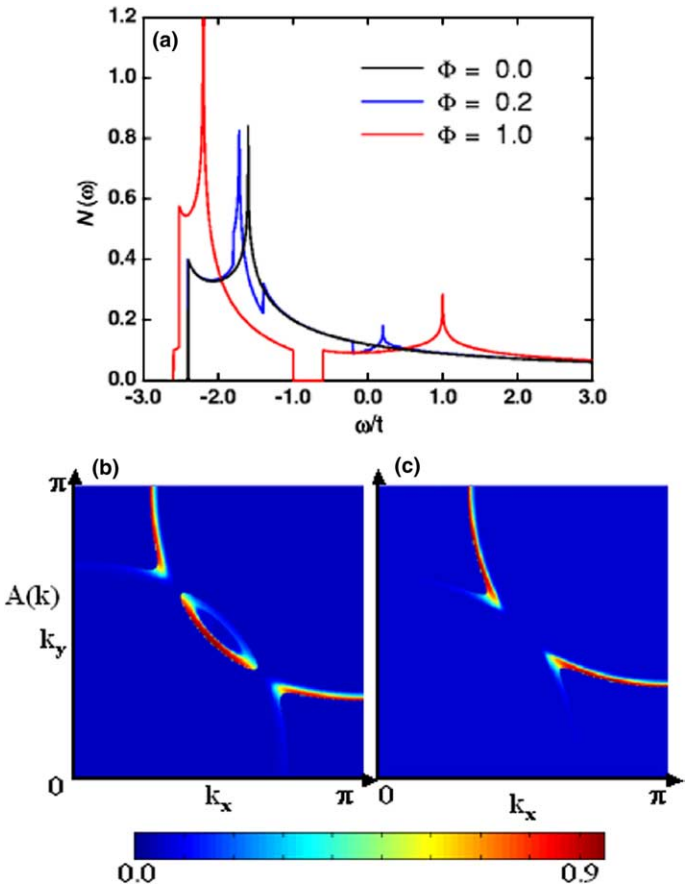

Fig. 1. Normal state DOS with SDW order $\Phi = 0$ (black), 0.2 (blue), and 1 (red) are shown in (a). The chemical potentials are set at zero. We will use $\Phi = 0.2$ for all calculations later in this paper. The near-Fermi-level spectral weight $A(\mathbf{k})$ (for $\Phi = 0.2$ and $\Delta_{SC} = 0.1$) are shown for the cases (b) $\mu = -0.3$ and (c) +0.1.

We now examine the low-temperature behavior of MPD. The MPD tensor $\lambda_{\mu\nu}(T)$ is related to the zero-momentum and zero-frequency current-current correlation function. The current operator can be written as

$$j_\mu(\mathbf{q}) = -e \sum_{\mathbf{k}\in \mathrm{MBZ}} \Psi^\dagger_{\mathbf{k}} \gamma_\mu \left(\mathbf{k} + \frac{\mathbf{q}}{2}\right) \Psi_{\mathbf{k}+\mathbf{Q}}, \tag{6}$$

where $\gamma_\mu(\mathbf{k}) \equiv \mathrm{Diag}[\mathbf{v}^\mu_{\mathbf{k}}\mathbf{1}_2, \mathbf{v}^\mu_{\mathbf{k}+\mathbf{Q}}\mathbf{1}_2]$, $\mathbf{v}^\mu \equiv \partial\xi_{\mathbf{k}}/\partial\mathbf{k}_\mu$, $\mathbf{1}_2 \equiv \mathrm{Diag}[1,1]$ is the 2×2 unit matrix, e is the electronic charge, and $\mathbf{k}$ is sum over the AF MBZ. $\lambda_{\mu\nu}(T)$ is then given by

$$\frac{1}{\lambda_{\mu\nu}(T)^2} = \frac{4\pi e^2}{\beta N} \sum_{\mathbf{k}, i\omega_n} \mathrm{Tr}\big[G^{\mathrm{SC}}(\mathbf{k}, i\omega_n)\gamma_\mu(\mathbf{k})G^{\mathrm{SC}}(\mathbf{k}, i\omega_n)\gamma_\nu(\mathbf{k}) - G^{\mathrm{N}}(\mathbf{k}, i\omega_n)\gamma_\mu(\mathbf{k})G^{\mathrm{N}}(\mathbf{k}, i\omega_n)\gamma_\nu(\mathbf{k})\big], \tag{7}$$

where G^{N} is the normal-state Green function matrix, which can be simply obtained from G^{SC} by setting Δ_{SC} to zero, but keeping the same SDW order Φ. Summing off the Matsubara frequencies, Eq. (7) is reduced to

$$\frac{1}{\lambda_{\mu\nu}(T)^2} = \frac{4\pi e^2}{N} \sum_{\mathbf{k}} \sum_{\eta\sigma\eta'\sigma'} \frac{f[E_{\eta\sigma}(\mathbf{k})] - f[E_{\eta'\sigma'}(\mathbf{k})]}{E_{\eta\sigma}(\mathbf{k}) - E_{\eta'\sigma'}(\mathbf{k})} \times \mathrm{Tr}\Big[a^{\mathrm{SC}}_{\eta\sigma}(\mathbf{k})\gamma_\mu(\mathbf{k})a^{\mathrm{SC}}_{\eta'\sigma'}(\mathbf{k})\gamma_\nu(\mathbf{k}) - (\Delta_{\mathrm{SC}} \to 0)\Big]. \tag{8}$$

Due to the tetragonal symmetry, $\lambda^{-2}_{\mu\nu} = \delta_{\mu\nu}\lambda^{-2}_{\mu\mu}$, and $\lambda_{xx} = \lambda_{yy} \equiv \lambda$. Some further simplification can be made and eventually this integral is evaluated numerically. The main contribution to the integral comes from the large $[f(\omega) - f(\omega')]/[\omega - \omega']$, i.e.,

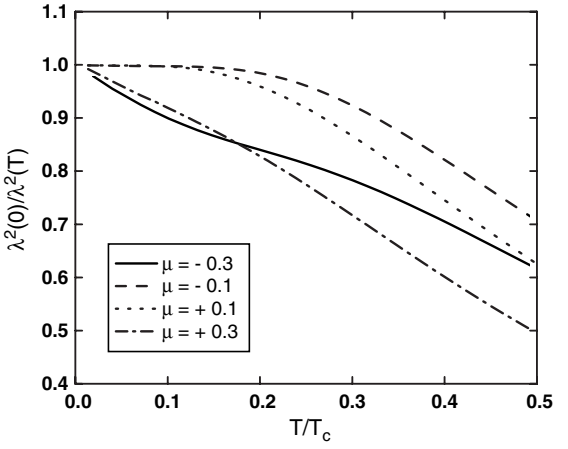

Fig. 2. Low-temperature magnetic penetration depth at various band fillings is plotted as $\lambda(0)^2/\lambda(T)^2$ versus the reduced temperature T/T_c ($2\Delta_{SC}/T_c = 4$ is used). The chemical potentials are $\mu = -0.3, -0.1, +0.1, +0.3$ (fillings from 1.16 to 1.30 for our band).

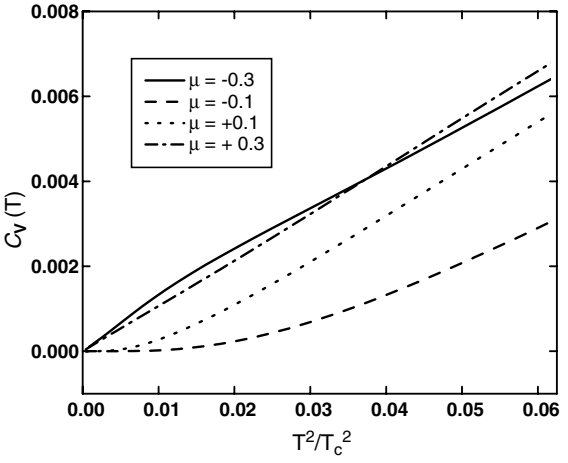

Fig. 3. The specific heat C_v is plotted versus T^2. The band parameters are the same as those in Fig. 2.

near-zero frequency regime, and it is therefore a sum over low-energy thermal excitations. When $\omega = \omega'$ (e.g., when $\eta = \eta'$ and $\sigma = \sigma'$), the quantity $[f(\omega) - f(\omega')]/[\omega - \omega']$ is defined as the limit $df/d\omega$.

Fig. 2 shows the low-temperature MPD. The same Δ_{SC} and Φ are used within the temperature range considered, and this approximation should be valid at least at the very low temperature regime, say below $T_c/4$. At approaching zero temperature, we find linearly decreasing behavior $\lambda(0)^{-2} - \lambda(T)^{-2} \propto T$ at low and high band fillings, which is essentially due to a nodal dSC; and negligible temperature dependence at some intermediate band fillings, which is due to a nodeless excitation gap in the single particle spectrum (see Fig. 4).

The transition between nodal-gap and full-gap behavior in the MPD is compared to the results of low-temperature specific heat. Fig. 3 shows the constant volume specific heat

$$C_v(T) = \frac{d}{dT}\sum_{\mathbf{k}\in MBZ,\eta\sigma} E_{\eta\sigma}(\mathbf{k}) f[E_{\eta\sigma}(\mathbf{k})] = 2\sum_{\mathbf{k}\in MBZ,\sigma} \frac{E_\sigma(\mathbf{k})^2}{T^2} f[E_\sigma(\mathbf{k})] f[-E_\sigma(\mathbf{k})], \quad (9)$$

where $df(\varepsilon)/dT = (\varepsilon/T^2) f(\varepsilon)\, f(-\varepsilon)$ is used in the second line. In congruence with the MPD, the T^2

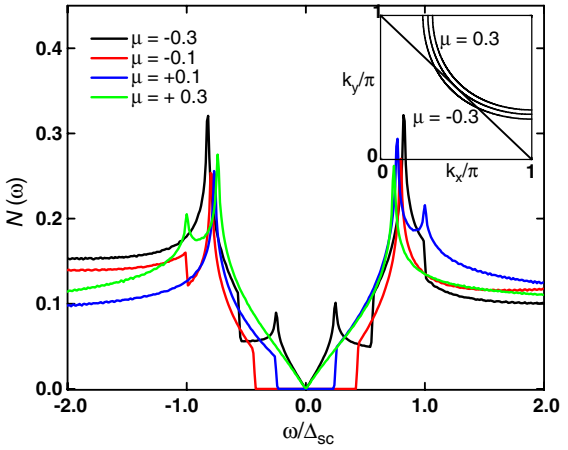

Fig. 4. The DOS in the SC state near the Fermi level is shown with chemical potentials $\mu = -0.3, -0.1, +0.1$, and $+0.3$. The inset shows the Fermi surfaces when there was no SDW order, at chemical potentials $\mu = -0.3, 0, +0.3$. The MBZ boundary is also shown.

dependence of $C_v(T)$ at low temperatures can be ascribed to the linear energy-dependence of the low-energy density of states (DOS) of the dSC (i.e., $N(\omega) \propto |\omega|$ at $\omega \sim 0$, see Fig. 4); and the case of negligible temperature-dependence is ascribable to a nodeless gap (see Fig. 4).

Fig. 4 shows the DOS [i.e., $N(\omega) = -(\pi N)^{-1}\sum_{\mathbf{k}} \mathrm{Im}[G^{SC}(\mathbf{k}, \omega + i0)]_{11}$] at different band

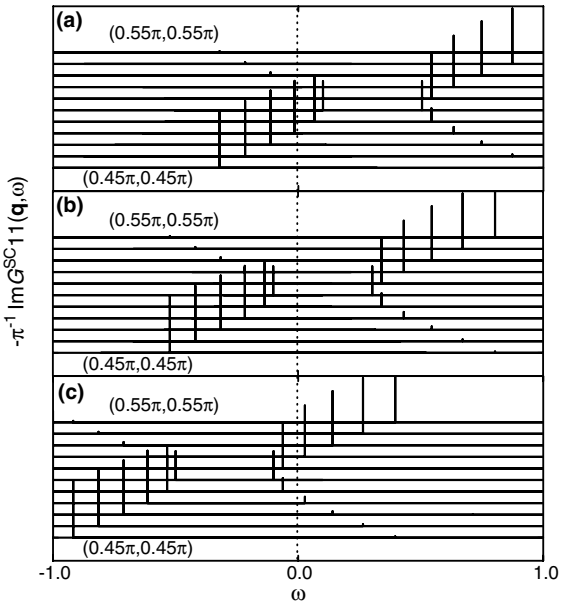

Fig. 5. Single-particle spectrum $-\pi^{-1}\mathrm{Im}[G^{\mathrm{SC}}(\mathbf{k},\omega + i0)]_{11}$ along the diagonal-$\mathbf{k}$ direction is plotted from $(0.45\pi, 0.45\pi)$ (lower most) to $(0.55\pi, 0.55\pi)$ (upper most), for (a) $\mu = -0.3$, (b) $\mu = -0.1$, and (c) $\mu = +0.3$. The heights of the spikes are drawn proportional to the weight of the poles.

fillings. The full gap [3] that appears at intermediate band fillings explains the small temperature dependence of λ (see Fig. 2) and C_{v} (see Fig. 3) at low temperatures. Interestingly, a subgap twin-peak structure [4] is seen in the case of the MBZ boundary cuts the FS but the gap remain nodal-like (the case of $\mu = -0.3$ in Fig. 4). Some "peak-dip-hump" structure may also appear (e.g., see the negative energy side of the $\mu = -0.1$ case in Fig. 4).

The formation of the full gap when the FS is close to the MBZ boundary is illucidated in Fig. 5. Fig. 5 shows the single-particle spectrum $-\pi^{-1}\mathrm{Im}[G^{\mathrm{SC}}(\mathbf{k},\omega + i0)]_{11}$ along the diagonal-$\mathbf{k}$ directions, where a plain $d_{x^2-y^2}$-wave SC system would have its gapless single-particle excitations. At the presence of a SDW, the diagonal-$\mathbf{k}$ QP peaks do not disperse to the Fermi level when the FS (defined at the absence of SDW) gets close to the MBZ boundary [Fig. 5(b). See also Fig. 1(c)], and this explains the full gaps in Fig. 4. Scattering by the SDW has opened up a gap at the vicinity of the MBZ boundary. Interestingly, since the ARPES can observe only the negative energy part of the single-particle spectrum, the QPs at the SC nodes that are gapped by a SDW [see Fig. 5(b)] may be seen to disperse like QPs that are gapped by a SC gap. Moreover, though the DOS may not vanish on the Fermi level, a forbidened window in ω-space at below the Fermi level may still be found for the diagonal-$\mathbf{k}$ QPs [see Fig. 4 and Fig. 5(c)].

3. Concluding remarks

We have used the same Δ_{SC}, T_{c}, and Φ throughout our discussion for simplicity. Taking into account the differences of those parameters in various cases should make no qualitative difference in our conclusions as we are essentially discussing thermally activated behaviors due to a full gap, or scale-less behaviors due to a nodal-like gap. As long as Φ is finite, there exists a range of doping (within the realistic doping regime) that can give rise to a full gap. Furthermore, we also believe that our conclusion will remain qualitatively the same when the vertex correction is taken into account, since the gap at the MBZ boundary will always be opened up due to the mixing of QPs at $\mathbf{k}$ and $\mathbf{k} + \mathbf{Q}$. As the would-be-gapless points on the FS get close to the MBZ boundary, they are pushed to higher energies and a full gap in the total DOS is formed.

We have adopted a phenomenological approach rather than obtaining the SDW order from a self-consistent mean-field-theory (MFT). This is because naive MFTs are usually insufficient to describe the very weak (probably incipient) but persisting SDW indicated by the experiments. In such a situation, the location of the FS but not the size of the SDW, is the dominant factor in

[3] Note that this full gap is not simply the SDW gap, as it is obviously much smaller than the SDW order $\Phi = 0.2$ chosen in this paper. It is due to the intertwined dSC and SDW order.

[4] Such subgap structure in the DOS resembles that of a $d_{x^2-y^2} + s$ gap (e.g., see Ref. [3]) or some sign-changing extended-s gap [e.g., see G. Zhao, Phys. Rev. B 64, (2001) 24503], which are essentially sign-changing gaps with more than one absolute magnitudes of gap maxima.

determining the low-energy excitations in the dSC state. Note that though we have assumed a static SDW, the result is in fact equally applicable to the case of an incipient SDW or a soft AF spin fluctuation, as the electrons around the Fermi level are "fast" modes, and any relatively "slow" spin fluctuations are essentially static.

Though the properties of the dSC state can be drastically modified at some of the band fillings, the normal state properties are expected to remain normal. For instance, the resistivity will always have a quadratic dependence on temperature because in the normal state there exists no gap in the DOS near the Fermi level [Fig. 1(a)]. On the impurity scattering effect on the MPD, the linear temperature dependence of $\lambda(T)^{-2}$ at low temperatures in the clean limit that occurs when the d-wave nodes on the FS are away from the MBZ boundary, is expected to cross over to quadratic in T (in the resonant scattering limit) [21], regardless of the existence of the SDW or not. The reason for the independence of SDW is that in those cases the low-energy nodal QPs are essentially unaffected—a fact that can be seen in the single-particle spectral function [see Fig. 5(a) and (c)], and manifested in the linear in $|\omega|$ dependence of the DOS at low energies (see Fig. 4). As the low-temperature MPD is related only to the low-energy excitations of those unaffected QPs, a theory including the effect of impurity scattering will be essentially the same as that without SDW, which is already widely available in literature [21].

At the overdoped compounds, two possible factors might account for the recovering of a nodal gap as seen in Ref. [10]. The first is, the diagonal portions of the FS have proceeded to the other side of, and leave the MBZ boundary (as studied in the current paper). The second is, the strength of the magnetic fluctuation is weakened. Precise ARPES and INS measurement on the compounds may be used to resolve the possibilities.

We have investigated the transmutation between nodal-gap-like and nodeless-gap-like behaviors in some of the electron-doped cuprates. A scenario inspired by experiments on some related compounds is proposed. We propose that there exists a weak or incipient SDW order in the compounds, and it is coupled to the QPs. This scattering can push the would-be-gapless diagonal QPs to higher energies, and a $d_{x^2-y^2}$-symmetry SC system can behave like it is nodeless.

Acknowledgment

This work is supported by the NSC of Taiwan under Grant No. 92-2112-M-009-035 (KKV) and 92-2112-M-003-009 (WCW). We thank C.-S. Ting for helpful discussion.

References

[1] D.J. van Harlingen, Rev. Mod. Phys. 67 (1995) 515.
[2] Y. Dagan et al., Phys. Rev. Lett. 87 (2001) 177004.
[3] N.-C. Yeh et al., Phys. Rev. Lett. 87 (2001) 87003.
[4] N.P. Armitage et al., Phys. Rev. Lett. 86 (2001) 1126.
[5] J.A. Skinta et al., Phys. Rev. Lett. 88 (2002) 207005.
[6] J.D. Kokales et al., Phys. Rev. Lett. 85 (2000) 3696.
[7] R. Prozorov et al., Phys. Rev. Lett. 85 (2000) 3700.
[8] D.H. Wu et al., Phys. Rev. Lett. 70 (1993) 85.
[9] A. Andreone et al., Phys. Rev. B 49 (1994) 6392.
[10] M.-S. Kim et al., Phys. Rev. Lett. 91 (2003) 87001.
[11] A. Kohen, G. Deutscher, <cond-mat/0207382>.
[12] D. Daghero et al., <cond-mat/0207411>.
[13] K.A. Muller, Phil. Mag. Lett. 82 (2002) 279.
[14] V.A. Khodel et al., <cond-mat/0307454>.
[15] H.J. Kang et al., Nature 423 (2003) 522.
[16] K. Yamada et al., Phys. Rev. Lett. 90 (2003) 137004.
[17] T.R. Thurston et al., Phys. Rev. Lett. 65 (1990) 263.
[18] N.P. Armitage et al., Phys. Rev. Lett. 87 (2001) 147003.
[19] A.P. Kampf, J.R. Schrieffer, Phys. Rev. B 42 (1990) 7967.
[20] B. Kyung et al., cond-mat/0312499.
[21] See, for example P. Arberg, M. Mansor, J.P. Carbotte, J. Phys. Chem. Solids 54 (1993) 1461.